Beyond kinetic relations

Lev Truskinovsky

Laboratoire de Mechanique des Solides, CNRS-UMR 7649, Ecole Polytechnique, 91128, Palaiseau, France

Anna Vainchtein *

Department of Mathematics, University of Pittsburgh, Pittsburgh, PA 15260, USA

Abstract

In this paper we discuss a new concept of a constitutive *kinetic equation* which represents a quasicontinuum analog of the conventional continuum mechanical concept of a *kinetic relation*. Kinetic relations link the velocity of the defect with the driving force and are widely used to model dynamical response of dislocations, cracks and phase boundaries. To illustrate the difference between kinetic relations and kinetic equations we consider a prototypical model of an overdamped defect in a one-dimensional lattice where all computations can be done explicitly. We show that in the strongly discrete limit the minimal kinetic equation is in fact a system of two ordinary differential equations involving the coordinate of the defect and another internal parameter describing the configuration of the core region.

1 Introduction

Kinetic relations associating a particular value of velocity with a given value of the driving force are widely used in continuum mechanics for the constitutive description of propagating lattice defects (e.g. phase boundaries, dislocations, cracks, etc. (Gurtin, 1999; Maugin, 1993). These, usually algebraic, relations form independent postulates which serve as closing macroscopic conditions. Since kinetic relations represent the vanishing core regions of the defects, they contain in a condensed form all information regarding the complex physical behavior at the microscale. In practice, kinetic relations are either taken

* Corresponding author
Email addresses: trusk@lms.polytechnique.fr (Lev Truskinovsky), aav4@pitt.edu (Anna Vainchtein).

from experiment or from the solutions of auxiliary microscale problems. In the macroscopic continuum description the core regions of the defects are represented by singularities, so that all the details of their interaction with localized inhomogeneities are lost. For instance, the velocity oscillations due to lattice discreteness and the corresponding pinning-depinning phenomena that generate intermittency become averaged out (Kardar, 1998).

To partially recover the missing information we propose to replace an algebraic relation between the macroscopic velocity of the defect and the corresponding macroscopic driving force by a *kinetic equation* linking the time derivatives of the effective parameters describing the microconfiguration of the core region with their local values and the value of the macroscopic driving force. Our approach can be viewed as an example of a multiscale (quasicontinuum) method aimed at bridging macroscopic continuum description outside the singularities with a more detailed atomistic resolution of the core regions (Tadmor et al., 1996; Li and E, 2005; Arndt and Luskin, 2008).

To illustrate the main idea of the approach we begin with a simple zero-dimensional example. Consider an overdamped dynamics of a material point in a one-dimensional configurational space:

$$\frac{\partial \nu}{\partial \tau} = -\frac{\partial \Phi(\nu, G(t))}{\partial \nu}, \tag{1}$$

where ν is a variable defining the microstate of the system, $G(t)$ is the slowly varying macroscopic driving force depending on slow time t. The fast time is defined as $\tau = t/\epsilon$ where $\epsilon << 1$ is a small parameter. We assume that the energy landscape $\Phi(\nu, G)$ is periodic in ν. The periodicity reflects micro-inhomogeneities due to lattice structure or imitates some other regular distribution of obstacles. We suppose that there exists an algebraic relation between the driving force G and the macroscopic velocity

$$V(t) = \left\langle \frac{\partial \nu}{\partial \tau} \right\rangle_\tau = \lim_{\epsilon \to 0} \epsilon \int_0^{1/\epsilon} \frac{\partial \nu}{\partial \tau} d\tau. \tag{2}$$

It can be written as $V(t) = V(G(t))$, and we interpret it as the macroscopic *kinetic relation*. For instance, if G prescribes a tilt of the simplest periodic energy landscape

$$\Phi(\nu, G) = G_{\mathrm{P}} \cos \nu - G\nu, \tag{3}$$

we obtain (e.g. Gruner et al., 1981)

$$V(G) = \begin{cases} 0 & |G| \le G_{\mathrm{P}} \\ \mathrm{sgn}(G - G_{\mathrm{P}})\sqrt{G^2 - G_{\mathrm{P}}^2} & |G| \ge G_{\mathrm{P}}. \end{cases} \tag{4}$$

In the realistic situations the microscopic description of the type (1) is very complex because it involves a huge number of variables and is too detailed.

In contrast, the *macroscopic description* of the type (4) is too schematic and cannot be trusted when one deals with the problems where slow and fast time scales cannot be separated. This point is often overlooked, and kinetic relations, implying adiabatic elimination of microscopic variables, are used in situations where both G and V are changing fast, as, for instance, in the cases of nucleation and depinning.

In this paper we propose to take a step back from the macroscopic level and return to the mesoscopic level where the algebraic kinetic relations can be replaced by the differential kinetic equations. These equations can be viewed as a low parametric representation of the full-scale atomistic (molecular dynamic) description of the type (1) which involves some specially selected collective variables characterizing the location of the defect and the structure of the core region. Kinetic equations are expected to describe the response of the core of the defect to relatively fast changes of the macroscopic driving force and when these changes are slow the kinetic equation must reduce to the kinetic relation. An example of such approach is provided by the rate and state-dependent constitutive laws in the theory of friction, where the set of internal state variables is assumed to satisfy differential constitutive relations (e.g. Rice and Ruina, 1983; Ruina, 1985). When such state variables are eliminated, one obtains in macroscopic variables an integral kinetic relation with nonlocal time dependence. This nonlocal kinetic relation becomes local only in the limit of sufficiently slow variation of the macroscopic parameters.

In what follows we present a detailed adaptation of these ideas to the case of martensitic phase transitions. Martensitic phase boundaries are particularly convenient for the demonstration of the main principles of our approach because these plane defects can be already adequately represented by one-dimensional models. To emphasize ideas we consider the simplest case of an isolated phase boundary with overdamped dynamics. At the microscale, the analysis of the steady propagation of a phase boundary requires a study of a dynamical system with an infinite number of degrees of freedom. At the macroscale the same defect can be modeled by a jump discontinuity whose evolution is determined from the conventional kinetic relation.

We pose the question of whether an intermediate description is possible when the interface is equipped with a small number of "mesoscopic" degrees of freedom whose dynamics reproduces the main effects of discreteness. An example of such a description in the theory of dislocations is provided by the representation of a static defect as an effective particle in equilibrium Peierls-Nabarro (PN) landscape (Braun and Kivshar, 2004). The static PN landscape is obtained by relaxing all microscopic variables other than one collective variable interpreted as the macroscopically observable location of the core. The idea of static PN landscape for a dislocation was extended to dynamics in the case when the discrete system is close to the continuum one. In this restricted set-

ting the dynamic PN landscape can be represented as the appropriately tilted static PN landscape (Hobart, 1965, 1966; Pokrovsky, 1981; Ishimori and Munakata, 1982; Ishibashi and Suzuki, 1984; Willis et al., 1986; Lazutkin et al., 1989; Flach and Kladko, 1996). Such approach, however, cannot be used in the strongly discrete case, when the dislocation core is narrow and the continuum approximation is not adequate (Joos, 1982; Furuya and de Almeida, 1987). In order to deal with the strongly discrete case it was proposed to trace the dynamics of the so-called "active points", which leads to the study of a low-dimensional dynamical system (Kladko et al., 2000; Carpio and Bonilla, 2003). So far the approach of "active points" has been applied to the modeling of dislocations only in the immediate vicinity of the depinning point.

In the present paper we extend the approach of "active points" to fast motions of martensitic phase boundaries and develop a systematic concept of a dynamic PN (DPN) landscape. Potentially, we search for a finite-dimensional center manifold type reduction of the original infinite-dimensional dynamical system, however in this paper we restrict our attention to the approximation of the traveling wave solutions only. The key to our approach is the assumption that during each period dynamics of only a few elastic elements located inside the core region around the phase boundary has to be resolved fully. The other elastic elements further away from the core region remain confined to their respective potential wells and their small adjustment to changing conditions can be treated as instantaneous. In contrast to the approach of kinetic relations here we need to follow not only the location but also the internal configuration of the front. Such extension of the scope is necessary because the core region of the defect is not translated with the center of mass as a rigid object but is instead experiencing periodic configurational deformations.

We apply this idea to an exactly solvable discrete lattice model with piecewise quadratic interaction potential. Using as a benchmark the exact traveling wave solution of the discrete problem for the steadily moving phase boundary (Truskinovsky and Vainchtein, 2005, 2008), we construct a simple two-dimensional dynamical system which generates a remarkably good approximation for the kinetics of the full infinite-dimensional system. The application of the obtained kinetic equations for the solution of the particular macroscopic boundary value problems involving strongly inhomogeneous media will be given elsewhere.

The paper is organized as follows. In Section 2 we formulate the singular macroscopic problem which requires a microscopic closure. To provide such a closure we turn to a specific microscopic model, represented by an overdamped chain with the interaction of nearest and next to nearest neighbors. In Section 3 we obtain an analytical traveling wave solution of the microscopic problem and extract from it the macroscopic kinetic relation. The construction of the classical static PN landscape and its utility for the modeling of dynamics are

discussed in Section 4. In Section 5 we build the simplest one-dimensional kinetic equation which gives rise to the simplest one-dimensional DPN landscape. We show, however, that the resulting one-dimensional kinetic equation is only adequate in the immediate vicinity of the depinning point. In Section 6 we replace it by a two-dimensional kinetic equation which works well in a larger interval of admissible velocities.

2 Macroscopic and microscopic models

Let $u(x,t)$ be the one-dimensional continuum displacement field. The macroscopic energy of a bar undergoing martensitic phase transition can be written as

$$\mathcal{E} = \int \left[\frac{\dot{u}^2}{2} + \phi(u_x) \right] dx. \tag{5}$$

Here the energy density $\phi(u_x)$ is represented by a double-well potential which will be specified later.

The dynamic equation corresponding to the energy (5) is

$$u_{tt} = (\hat{\sigma}(u_x))_x, \tag{6}$$

where $u_t \equiv \partial u/\partial t$ is the macroscopic velocity and $u_x \equiv \partial u/\partial x$ is the macroscopic strain and $\hat{\sigma}(u_x) = \phi'(u_x)$. On discontinuities, the equation (6) is usually supplemented with the appropriate jump conditions. Let f_- and f_+ denote the values of $f(x)$ to the left and to the right of the interface, and introduce the notations $[\![f]\!] \equiv f_+ - f_-$ for the jump and $\{f\} \equiv (f_+ + f_-)/2$ for the average of f across the discontinuity. Then the parameters on a discontinuity must satisfy the classical Rankine-Hugoniot jump conditions

$$[\![u_\tau]\!] + V[\![u_x]\!] = 0, \quad V[\![u_\tau]\!] + [\![\hat{\sigma}(u_x)]\!] = 0. \tag{7}$$

The entropy inequality, which is also typically assumed to hold, takes the form

$$\mathcal{R} = GV \geq 0, \tag{8}$$

where $\mathcal{R}$ is the rate of energy dissipation and

$$G = [\![\phi]\!] - \{\hat{\sigma}(u_x)\}[\![u_x]\!] \tag{9}$$

is the configurational (driving) force.

Imposing the entropy inequality is sufficient for local uniqueness in the case of supersonic discontinuities (shock waves). In the case of subsonic phase boundaries, in order to obtain a unique solution one must specify the rate of entropy production as well. This is usually done phenomenologically through

the kinetic relation $G = G(V)$ between the driving force and the velocity (Truskinovsky, 1987; Abeyaratne and Knowles, 1991). The specification of the microscopic model allows one in principle to compute the function $G(V)$ from the microscopic traveling wave solution (Truskinovsky, 1982; Slemrod, 1983).

As an example of a microscopic theory generating a particular kinetic relation consider an infinite chain of particles, connected to their nearest neighbors (NN) through viscoelastic springs and to their next-to-nearest neighbors (NNN) by elastic springs (see Figure 1). Suppose that in the undeformed configuration the NN and NNN springs have lengths ε and 2ε, respectively. Let $u_n(t)$ denote the displacement of nth particle at time t with respect to the reference configuration. The deformation of nth NN spring is measured by its strain

$$w_n = \frac{u_n - u_{n-1}}{\varepsilon}. \tag{10}$$

For the viscoelastic NN springs we assume the following constitutive relation:

$$f_{\rm NN}(w, \dot{w}) = \phi'_{\rm NN}(w) + \xi \dot{w}, \tag{11}$$

where $\xi > 0$ is the viscosity coefficient accounting for dissipation which may be due to the presence of internal degrees of freedom that are not accounted for in this model. To generate domain boundaries we need $\phi_{\rm NN}(w)$ to be at least a double-well potential; to obtain explicit solutions, we shall also assume that this function is biquadratic:

$$\phi_{\rm NN}(w) = \begin{cases} \frac{1}{2}Kw^2, & w \le w_c \\ \frac{1}{2}K(w-a)^2 + Ka\left(w_c - \frac{a}{2}\right), & w \ge w_c. \end{cases} \tag{12}$$

One can see that under these assumptions the NN elastic units can be in two different phases, depending on whether the strain is below (phase I) or above (phase II) the critical value w_c. The parameter a measures the transformation strain. To simplify the calculations, we assumed that the elastic moduli in the NN phases are the same and that the NNN interactions are linearly elastic:

$$f_{\rm NNN}(\hat{w}) = 2\gamma\hat{w}. \tag{13}$$

Here we defined $\hat{w}_n = \frac{1}{2}(w_{n+1}+w_n)$ as the strain in the NNN spring connecting $(n+1)$th and $(n-1)$th particles.

The dynamics of the chain is governed by the following system of equations

$$\begin{aligned} \rho\varepsilon\ddot{u}_n =& K[w_{n+1} - w_n - \theta(w_{n+1} - w_c)a + \theta(w_n - w_c)a] \\ &+ \gamma(w_{n+2} + w_{n+1} - w_n - w_{n-1}) + \xi(\dot{w}_{n+1} - \dot{w}_n), \end{aligned} \tag{14}$$

where ρ is the mass density of the chain and $\theta(x)$ is a unit step function. To ensure stability of the chain in the undeformed configuration, we must require

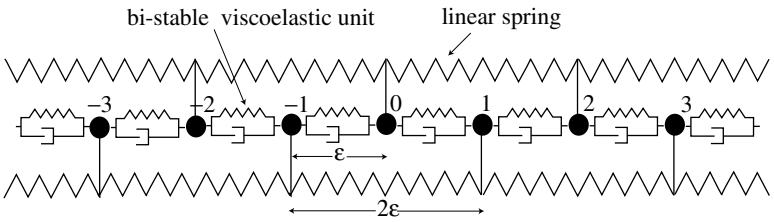

Fig. 1. The discrete microstructure with viscoelastic nearest and elastic next-to-nearest-neighbor interactions.

that

$$E = K + 4\gamma > 0, \tag{15}$$

where E is the homogenized macroscopic elastic modulus; following Truskinovsky and Vainchtein (2003, 2004), we also assume that the NNN interactions are of ferromagnetic type, meaning that $\gamma \leq 0$.

There are two time scales associated with this problem: the time scale of inertia, $T_{\text{in}} = \varepsilon\sqrt{\rho/E}$, and the viscosity time scale, $T_{\text{visc}} = \xi/E$. In this paper we consider the overdamped limit when $T_{\text{visc}} >> T_{\text{in}}$, i.e.

$$\xi >> \varepsilon\sqrt{\rho E}. \tag{16}$$

We can now rescale the problem using T_{visc} as the time scale and letting

$$\bar{t} = tE/\xi, \quad \bar{u} = \frac{u}{\Delta\varepsilon}, \quad \bar{w} = \frac{w}{\Delta}, \quad \bar{w}_c = \frac{w_c}{\Delta}, \tag{17}$$

where we defined the macroscopic transformation strain

$$\Delta = \frac{aK}{E}. \tag{18}$$

Dropping the bars on the new variables, we obtain the dimensionless equations for the overdamped dynamics of the chain:

$$\dot{w}_n - \dot{w}_{n+1} = \hat{\sigma}(w_{n+1}) - \hat{\sigma}(w_n) + D(w_{n+2} + w_{n+1} - w_n - w_{n-1}), \tag{19}$$

where

$$\hat{\sigma}(w) = w - \theta(w - w_c) \tag{20}$$

is the homogenized stress-strain law. The dimensionless parameter

$$D = -\frac{\gamma}{E} \geq 0, \tag{21}$$

measures the relative strength of NN and NNN interactions. In what follows it will also be interpreted as a measure of coupling of the bistable units.

Observe that equation (19) can be "integrated", yielding

$$\dot{w}_n = D(w_{n+1} - 2w_n + w_{n-1}) - \hat{\sigma}(w_n) + \sigma. \tag{22}$$

Here the integration constant σ has the meaning of the applied force. One can see that equation (22) resembles the discrete overdamped Frenkel-Kontorova equation which is used in many applications (Fáth, 1998; Keener, 1987; Carpio and Bonilla, 2003; Kresse and Truskinovsky, 2007); a subtle but important distinction of equation (19) is that the coupling coefficient D is independent of ε.

To place the microscopic equation (22) in the gradient flow framework of (1) we can rewrite it as

$$\dot{\mathbf{w}} = -\nabla \mathcal{W}(\mathbf{w}; G), \tag{23}$$

where $\mathbf{w} \in \mathbb{R}^\infty$ is the vector of strains, the gradient is taken with respect to $\mathbf{w}$, and

$$\mathcal{W} = \sum_{n=-\infty}^{\infty} \left(\frac{1}{2} w_n^2 - (w_n - w_c)\theta(w_n - w_c) + D(w_{n+1} - w_n)^2 - (\sigma_{\mathrm{M}} + G) w_n \right), \tag{24}$$

is the dimensionless energy of the system. Our main goal will be to approximate the infinite-dimensional dynamical system (23) by a finite-dimensional reduced dynamical system of the type

$$\dot{\boldsymbol{\nu}} = -\boldsymbol{\alpha} \nabla \Phi(\boldsymbol{\nu}; G), \tag{25}$$

where $\boldsymbol{\alpha}$ is the effective mobility matrix and the gradient is taken with respect to the order parameter $\boldsymbol{\nu} \in \mathbb{R}^K$. The integer-valued parameter K defines the dimensionality of the reduced system. After the solution of the vector equation (25) is known, the approximation of the discrete field (23) should be recoverable from the relations $w_n = w_n(\nu_1, \ldots, \nu_K)$ describing adiabatic relaxation of the 'non-order-parameter' variables.

In what follows, instead of attempting a general reduction of (23) to (25) we focus only on the approximation of the particular solutions of (23) of the type $w_n(t) = w(n - V(G)t)$ describing propagating phase boundaries. Here the unknown function $V(G)$ defines the conventional kinetic relation, which should, of course, be compatible with (23).

3 Traveling wave solution of the microscopic problem

To construct a benchmark traveling wave solution of the system (22) we assume that

$$w_n(t) = w(\eta), \quad \eta = n - Vt, \tag{26}$$

where V is the dimensionless velocity of the front, which represents a moving phase boundary. Suppose that our solution describes an isolated phase

boundary that leaves phase II behind, i.e.

$$w(\eta) < w_c \quad \text{for } \eta > 0, \qquad w(\eta) > w_c \quad \text{for } \eta < 0 \tag{27}$$

Under these assumptions, (22) reduces to

$$Vw'(\eta) - D(w(\eta+1) - 2w(\eta) + w(\eta-1)) + w(\eta) = \theta(-\eta) + \sigma \tag{28}$$

At infinity the solution must tend to uniform-strain equilibria of (19):

$$w(\eta) \to w_\pm \quad \text{as } x \to \pm\infty. \tag{29}$$

Finally, for consistency, we must also require that

$$w(0) = w_c. \tag{30}$$

Since the equation (28) is linear, we can be solve it using Fourier transform (see Carpio and Bonilla, 2003; Fáth, 1998; Truskinovsky and Vainchtein, 2008, for details). We obtain

$$w(\eta) = \begin{cases} \sigma + 1 + \sum\limits_{k \in S^-(V)} \dfrac{e^{ik\eta}}{k\Lambda_k(k,V)} & \text{for } \eta < 0 \\ \sigma - \sum\limits_{k \in S^+(V)} \dfrac{e^{ik\eta}}{k\Lambda_k(k,V)} & \text{for } \eta > 0, \end{cases} \tag{31}$$

where $S^\pm(V) = \{k : \Lambda(k,V) = 0,\ \mathrm{Im}k \gtrless 0\}$ are the sets of roots of the dispersion relation

$$\Lambda(k,V) \equiv 1 + 4D\sin^2(k/2) - Vik = 0.$$

Continuity of $w(\eta)$ at $\eta = 0$ gives the relationship between the applied stress and velocity of the traveling wave:

$$\sigma = \sigma_M + \frac{1}{2} + \sum_{k \in S^+(V)} \frac{1}{k\Lambda_k(k,V)} = \sigma_M - \frac{1}{2} - \sum_{k \in S^-(V)} \frac{1}{k\Lambda_k(k,V)}, \tag{32}$$

where

$$\sigma_{\mathrm{M}} = w_c - 1/2 \tag{33}$$

is the Maxwell stress. The difference between applied and Maxwell stresses is equal to the driving force $G = \sigma - \sigma_{\mathrm{M}}$ (see Truskinovsky and Vainchtein, 2005), and we thus obtain the desired kinetic relation

$$G(V) = \frac{1}{2} + \sum_{k \in S^+(V)} \frac{1}{k\Lambda_k(k,V)}. \tag{34}$$

The structure of the kinetic relation for different values of D is illustrated in Figure 2. One can see that at $D = 0$ (no NNN interactions) the driving

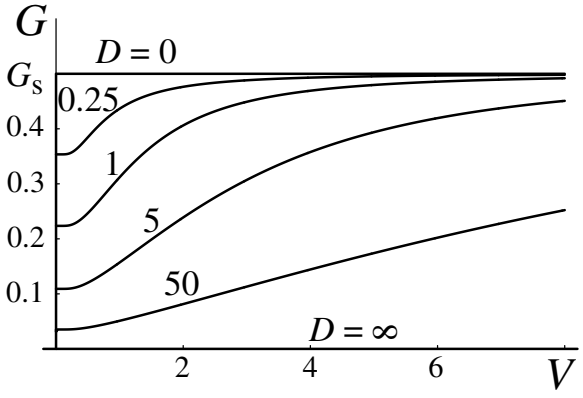

Fig. 2. Kinetic relation for different values of D.

force (34) must be constant for all $V > 0$ and equal to the spinodal value $G = G_{\rm S} = 1/2$; at $V = 0$ it can take any value between 0 and $G_{\rm S}$. In the other limit of $D = \infty$ the driving force becomes equal to zero at all values of V. In between these limits the complex roots in the set $S^+(V)$ tend to infinity at large V and the kinetic curves approach the common limit corresponding to $D = 0$ so that G tends to $G_{\rm S}$. At $D > 1/12$ the large-velocity discrete kinetics is well approximated by the formula (Truskinovsky and Vainchtein, 2008)

$$G(V) = \frac{V}{2\sqrt{V^2 + 4D - 1/3}},$$

which describes the kinetics of the overdamped viscosity-capillarity model governed by the partial differential equation $w_t = (D - 1/12)w_{xx} - \hat{\sigma}(w) + \sigma$.

For later comparison we need to know in more detail the zero-velocity asymptotics of the kinetic relation (34). As V tends to zero from above, the driving force approaches the Peierls threshold $G(0+) = G_{\rm P}$. To compute the function $G_{\rm P}(D)$ we recall that at $V = 0$ the continuous variable $\eta = n - Vt$ takes discrete values, and the strain profile (31) becomes discontinuous at every integer η. The differential equation reduces to a system of finite-difference equations, and we can replace the continuous Fourier transform by its discrete analog (Celli and Flytzanis, 1970; Kresse and Truskinovsky, 2003; Slepyan, 1982; Truskinovsky and Vainchtein, 2005). Both this procedure and direct solution of the difference equations yield the following family of equilibrium solutions, with a phase boundary at $n = m$ (Fáth, 1998; Hobart, 1965; Truskinovsky and Vainchtein, 2003):

$$w_n^m(G) = \sigma_{\rm M} + \begin{cases} G + 1 - \dfrac{\exp(\lambda(n - m - 1/2))}{2\cosh(\lambda/2)}, & n < m \\ G + \dfrac{\exp(-\lambda(n - m - 1/2))}{2\cosh(\lambda/2)}, & n \geq m, \end{cases} \tag{35}$$

parameterized by the driving force $G = \sigma - \sigma_{\rm M}$. Here

$$\lambda(D) = \operatorname{arccosh}\left(1 + \frac{1}{2D}\right). \tag{36}$$

The admissibility constraints

$$w_n^m \geq w_c \quad \text{for } n \leq m, \qquad w_n^m \leq w_c \quad \text{for } n \geq m+1 \tag{37}$$

determine the constraints on G; the set of driving forces satisfying these constraints constitutes the *trapping region*. One can show that for $D > 0$ the strain profile (35) is monotone, so the constraints (37) can be replaced by $w_m^m \geq w_c$ and $w_{m+1}^m \leq w_c$. The trapping region is then given by

$$|G| \leq G_{\rm P}, \tag{38}$$

where

$$G_{\rm P}(D) = \frac{1}{2}\tanh\frac{\lambda}{2} = \frac{1}{2\sqrt{1+4D}}. \tag{39}$$

is the desired expression for the Peierls threshold (see also Braun et al., 1990; Truskinovsky and Vainchtein, 2003).

The general behavior of the traveling wave solutions in the range of small velocities V is known from the studies of discrete reaction-diffusion equation (see, for example, Carpio and Bonilla, 2003; Fáth, 1998, and references therein). Thus one can show that in the limit $V \to 0+$ the traveling wave solution approaches the staircase profile:

$$w^{V\to 0+}(\eta) = w_c + \frac{e^{\lambda/2}}{2\cosh(\lambda/2)} - \tanh(\lambda/2)\left(\theta(\eta) + \sum_{p=1}^{\infty}[\theta(\eta+p)+\theta(\eta-p)]e^{-\lambda p}\right). \tag{40}$$

Direct evaluation shows that for $n \leq \eta < n+1$ the limiting solution is given by the saddle-point equilibrium (35) corresponding to $G = G_{\rm P}$ and $m = 0$:

$$w^{V=0+}(\eta) = w_n^{-1}(G_{\rm P})$$

Note that in this solution the 0th NN spring has the critical strain: $w_0^{-1}(G_{\rm P}) = w_c$.

As we increase V, the staircase structure smoothens out. The small-V solutions represent a singular perturbation of the solution $w^{V=0+}(\eta)$ characterized by the opening of the thin boundary layers which scale with V. During each period $T = 1/V$ the dynamics can be visualized as an approach toward the closest "virtual attractor" $s_n^m(G) = w_n^{m-1}(G)$, where the expression (35) for the equilibrium state is used formally for "forbidden" values of G outside the trapping region (38) where the constraints (37) are violated (Fáth, 1998). This corresponds to extending the parabolas beyond the critical strain w_c.

The virtual state satisfies the inequalities $s_n^m > w_c$ for $n \le m$ and $s_n^m \le w_c$ for $n \ge m+1$. In particular, $s_m^m = w_c + G - G_{\rm P} > w_c$ for $G > G_{\rm P}$. The virtual attractor is never reached, because as soon as one of the strains reaches the value w_c, the system deviates toward the next virtual state, and so on.

Now suppose that $G > G_{\rm P}$ and that it is the 0th spring which has the critical strain. Then the closest virtual attractor is s_n^1. Following Fáth (1998), we set

$$w_n = s_n^1 - \delta w_n$$

and obtain the system of linear equations

$$\delta\dot{w}_n = D(\delta w_{n+1} - 2\delta w_n + \delta w_{n-1}) - \delta w_n, \tag{41}$$

which describes the approach toward the virtual attractor. Consider the following initial condition:

$$w_n(0) = w_c - \frac{1}{2} + G + \begin{cases} 1 - (G+\frac{1}{2})e^{\lambda n}, & n \le 0 \\ (\frac{1}{2} - G)e^{-\lambda n} & n \ge 1, \end{cases}$$

which sets $w_0(0) = w_c$ and minimizes the energy with respect to all other NN strains. Notice that the 0th strain starts exactly at the critical value as the descent toward s_n^1 begins. Recalling (35) and the fact that $s_n^1(G) = w_n^0(G)$, we get

$$\delta w_n(0) = s_n^1(G) - w_n(0) = (G + G_{\rm P})e^{-\lambda|n|}. \tag{42}$$

Using the Green's function for (41) derived by Fáth (1998), we obtain the solution of (41) subject to the initial condition (42):

$$\delta w_n(t) = (G + G_{\rm P})\Sigma_n(2Dt)e^{-(1+2D)t}, \tag{43}$$

where

$$\Sigma_n(\tau) = \sum_{m=-\infty}^{\infty} e^{-\lambda|m|} I_{n-m}(\tau)$$

in terms of the Bessel function $I_n(\tau) = \frac{1}{\pi}\int_0^\pi e^{\tau\cos\theta}\cos(n\theta)d\theta$. The solution (43) is valid until $t = 1/V$, when w_1 reaches the critical strain: $w_1(1/V) = s_1^1(G) - \delta w_1(1/V) = w_c$. This yields a new approximate kinetic relation

$$G(V) = G_{\rm P}\frac{1 + e^{-(1+2D)/V}\Sigma_1(2D/V)}{1 - e^{-(1+2D)/V}\Sigma_1(2D/V)} \tag{44}$$

At small D the approximation is very good for all V and yields the correct large-V asymptotics ($G \to 1/2$). Observing that at small V

$$\Sigma_1(2D/V) \approx \frac{\sqrt{V}e^{2D/V}}{2G_{\rm P}\sqrt{4\pi D}},$$

we obtain that up to the terms of order $Ve^{-2/V}$

$$G - G_{\rm P} \approx \frac{\sqrt{V}\exp(-1/V)}{\sqrt{4\pi D}}. \tag{45}$$

This small-V asymptotics, first obtained by Fáth (1998) using a different initial condition, is due to the degenerate nature of the bilinear model; for smoother $\hat{\sigma}(w)$ the scaling is known to be parabolic, $G - G_{\rm P} \sim V^2$, as in a typical saddle-node bifurcation (Carpio and Bonilla, 2003).

4 Classical PN landscape

We begin the development of the systematic reduction procedure by trying to approximate kinetic relations around $V = 0$ where the kinetic equation type description has been traditionally attempted in terms of the tilted Peierls-Nabarro (PN) energy landscape. For the present model the static PN landscape was first obtained by Truskinovsky and Vainchtein (2003), and we begin with a brief review of the construction.

We recall that at $|G| \le G_{\rm P}$ the phase boundary can occupy an infinite set of stable equilibrium states given by (35). In order to link these stable states one can choose a particular path involving non-equilibrium intermediate configurations. For instance, consider two equilibrium configurations, one with the phase boundary located at $n = i - 1$ and the other one at $n = i$. Suppose for determinacy that $0 \le G \le G_{\rm P}$ and assume that phase II is located behind the phase boundary. Consider all paths connecting the two equilibria along which the ith NN spring is the only one that changes phase, while all other springs stay in their respective phases. As the ith NN spring crosses the critical value of strain w_c to switch phases, each path goes through an energy barrier.

Among all such paths, we can select the energetically preferred PN path that involves the minimal energy barrier. This is achieved by minimizing the energy of the chain with respect to all strains w_k with $k \neq i$ for a given w_i:

$$(1+2D)w_k - D(w_{k+1} + w_{k-1}) = \sigma_{\rm M} + \begin{cases} G+1, & k \le i-1 \\ G, & k \ge i+1. \end{cases} \tag{46}$$

Note that this amounts to adiabatic elimination of all degrees of freedom except the strain of the ith NN spring, which can be viewed as an order parameter along the path. One can show (Truskinovsky and Vainchtein, 2003, 2004) that the resulting path necessarily goes through the saddle point in the energy landscape (where $w_i = w_c$), and hence the energy barrier is minimal.

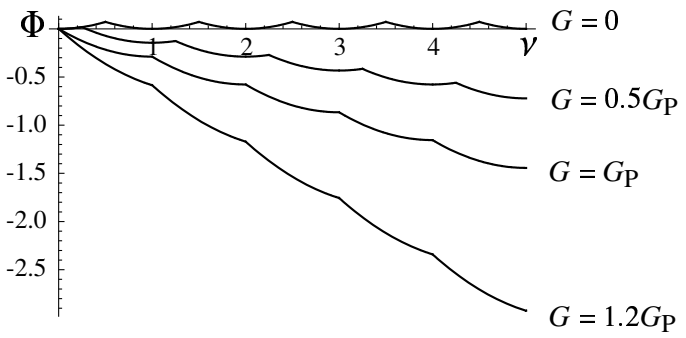

Fig. 3. One-dimensional energy landscape $\Phi(\nu; G)$ at $D = 0.5$ and different G. The classical static PN landscape corresponds to $G \leq G_{\rm P}$. The dynamic potential above the Periels threshold $G > G_{\rm P}$ was constructed using the $K = 1$ approximation.

Solving equations (46) at $k \leq i-1$ and $k \geq i+1$ and requiring that the corresponding solutions, when extended to $k = i$, both equal w_i, we obtain

$$w_k = \sigma_{\rm M} + \begin{cases} G + 1 + e^{\lambda(k-i)}(w_i - \sigma_{\rm M} - G - 1), & k \leq i \\ G + e^{-\lambda(k-i)}(w_i - \sigma_{\rm M} - G), & k \geq i. \end{cases} \tag{47}$$

Along the path the order parameter w_i increases from its value in the first minimum,

$$w_{\rm L} = w_i^{i-1}(G) = \sigma_{\rm M} + G + \frac{\exp(-\lambda/2)}{2\cosh(\lambda/2)} \leq w_c,$$

to the one in the second minimum:

$$w_{\rm U} = w_i^{i}(G) = \sigma_{\rm M} + G + 1 - \frac{\exp(-\lambda/2)}{2\cosh(\lambda/2)} \geq w_c,$$

while going through the saddle point $w_i = w_c$, where the energy along this path reaches its maximal value (due to the nonsmoothness of the biquadratic potential at $w = w_c$, the local maxima of the energy landscape correspond to singular points). We now proceed to construct a path that connects not just two but all equivalent equilibrium points and can be viewed as an advance of an isolated phase boundary. To this end we replace the order parameters w_i which were operative in each consecutive segment of the path by a global order parameter ν defined implicitly by

$$w_{[\nu]} = w^*(\nu) = \sigma_{\rm M} + G + \frac{\exp(-\lambda/2)}{2\cosh(\lambda/2)} + (\nu - [\nu])\tanh(\lambda/2), \tag{48}$$

where $[\nu]$ denotes the integer part of ν (the largest integer less than ν). At the integer values of ν we have $w_{[\nu]} = w_{\rm L}$, and as ν approaches $[\nu]+1$ from below, $w_{[\nu]}$ linearly increases to $w_{\rm U}$. The function $w^*(\nu)$ is periodic with period 1 and has jump discontinuities at $\nu = [\nu]$. One can see that ν can be interpreted as the macroscopic location of the interface (the particle in our effective model) as it moves through the lattice.

Using (48) and recalling (47), we obtain the one-parameter solution path parametrized by ν:

$$w_k = \sigma_M + \begin{cases} G + 1 + e^{\lambda(k-[\nu])}(w^*(\nu) - \sigma_{\rm M} - G - 1), & k \le [\nu] \\ G + e^{-\lambda(k-[\nu])}(w^*(\nu) - \sigma_{\rm M} - G), & k \ge [\nu]. \end{cases} \tag{49}$$

The next step is to evaluate the energy $\mathcal{W}$ along the path (49). For the infinite system we need to use the renormalized quantity $\Phi(\nu; G) = \mathcal{W}(\nu) - \mathcal{W}(0)$. Substituting (49) in (24), we obtain for $0 \le G \le G_{\rm P}$:

$$\Phi(\nu; G) = G_{\rm P}(\nu - [\nu])^2 - G[\nu] - (G - G_{\rm P} + 2(\nu - [\nu])G_{\rm P})\theta\left(\nu - [\nu] - \frac{G_{\rm P} - G}{2G_{\rm P}}\right). \tag{50}$$

The minima of $\Phi(\nu; G)$ are located at the integer values of ν and correspond to stable equilibrium states, while the singularities at $\nu = \nu_i$ represent unstable equilibria where $w_i(\nu_i) = w_c$ (see Fig. 3).

The energy barrier separating the equilibria at $\nu = i$ and $\nu = i + 1$ is independent of i and equals

$$\mathcal{B} \equiv \Phi(\nu_i) - \Phi(i) = \frac{(G_{\rm P} - G)^2}{4G_{\rm P}}.$$

At $G = G_{\rm P}$ the lower bound of $w_{[\nu]}$ reaches the critical value, $w_{\rm L} = w_c$, and the equilibria become marginally stable; see the curve $G = G_{\rm P}$ in Fig. 3. Above the Peierls threshold ($G_{\rm P} < G < G_{\rm S}$), there are no equilibria, and the above construction is no longer valid.

One very approximate but rather common way to extend the idea of PN landscape beyond $G = G_{\rm P}$ is to take the classical PN landscape at $G = 0$ (Maxwell stress) and tilt it (Braun and Kivshar, 2004). More precisely, we can define

$$\Phi_{\rm T}(\nu; G) = \Phi(\nu + 1/2; 0) - G\nu - \frac{G_{\rm P}}{4}, \tag{51}$$

where we have also added a constant to ensure that $\Phi_{\rm T}(0; G) = 0$. It is not hard to see that at $G \le G_{\rm P}$ the energy (50) agrees with (51) up to the appropriate shifts in horizontal and vertical directions:

$$\Phi\left(\nu + \frac{G_{\rm P} - G}{2G_{\rm P}}; G\right) - \frac{(G_{\rm P} - G)^2}{4G_{\rm P}} = \Phi_{\rm T}(\nu; G), \quad 0 \le G \le G_{\rm P}.$$

The two landscapes coincide exactly only at the Peierls threshold and differ below this threshold. Thus, in (50) the local energy minima are always located at the integer values of ν, reflecting the fact that in a discrete system position of a phase boundary coincides with a lattice point, and the points of local maxima move toward the integer values as G increases until at $G = G_{\rm P}$ the

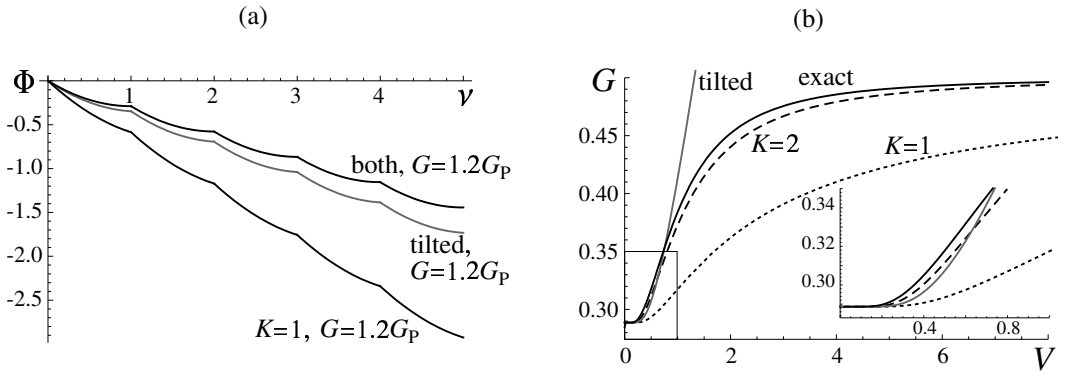

Fig. 4. (a) The tilted energy landscape (grey) and the DPN landscape for $K = 1$ (black) at $D = 0.5$. The two landscapes coincide at $G = G_{\rm P}$. (b) The exact kinetic relation $G(V)$ (solid curve) and its approximations via the tilted landscape (grey curve), $K = 1$ approximation (dotted curve) and $K = 2$ approximation (dashed curve).

minumum and maximum points merge. Meanwhile, in the case of the tilted PN landscape (51) the local maxima are always fixed at the integer values, and the minimum points move instead.

Now, since the tilted landscape can be extended beyond the Peierls threshold $G = G_{\rm P}$ we can try to model the dynamics of our phase boundary by the overdamped motion of a particle in this landscape (see the grey curve in Figure 4a). The equation of motion takes the form

$$\dot{\nu} = -\alpha\Phi'_{\rm T}(\nu; G) = -\alpha(2G_{\rm P}(\nu - [\nu] - 1/2) - G).$$

Solving this equation subject to the condition $\nu([Vt]/V) = [Vt]$ yields

$$\nu(t) = [Vt] + \frac{G + G_{\rm P}}{2G_{\rm P}}\left(1 - e^{-2\alpha G_{\rm P}(t-[Vt]/V)}\right).$$

Imposing $\nu(([Vt]+1)/V) = [Vt]+1$, we obtain the kinetic relation

$$G(V) = G_{\rm P}\frac{1 + e^{-2\alpha G_{\rm P}/V}}{1 - e^{-2\alpha G_{\rm P}/V}}. \qquad (52)$$

Expectedly, it gives the correct limit $G \to G_{\rm P}$ when $V \to 0$. However, in contrast to the discrete kinetic equation (34) the function (52) is unbounded: at large V, we have $G(V) \approx V/\alpha$ (see Figure 4b). In addition, since the physical meaning of the dynamic variable $\nu(t)$ is obscure, it is not clear how one can recover the strains $w_n(t)$.

5 One-dimensional DPN landscape (K=1)

We now take a more systematic point of view on how the idea of classical PN landscape can be extended to dynamics. We begin with the $K = 1$ approximation which means that we choose a scalar collective variable whose dynamics we follow faithfully while minimizing the energy with respect to all remaining variables. Our choice of the order parameter is motivated by the "single-active-site theory" (Kladko et al., 2000; Carpio and Bonilla, 2003). More precisely, we assume that the motion is periodic and during each period only a single NN spring, located right behind the phase transition front and actually changing the energy well during this period, is important.

Thus, suppose that at $t = 0$ the 0th NN spring has just switched to phase II: $w_0(0) = w_c$. Therefore, during the time period $0 \le t < 1/V$ the "active strain" is w_0. Minimizing the energy with respect to all other strain variables, we obtain

$$w_n = w_c - 1/2 + G + \begin{cases} 1 + (w_0 - w_c - G - 1/2)e^{\lambda n}, & n \le 0 \\ (w_0 - w_c - G + 1/2)e^{-\lambda n} & n \ge 1. \end{cases} \tag{53}$$

Substituting these expressions in (22) for $n = 0$ with $\hat{\sigma}(w)$ given by (20), we obtain a single equation governing the dynamics of the active point:

$$\dot{w}_0 = -w_0\{1 + 2D(1 - e^{-\lambda})\} + w_c + G + 1/2 + 2D(G + w_c)(1 - e^{-\lambda}). \tag{54}$$

This is a prototype of our kinetic equation. To see whether it is compatible with exact kinetic relation (34), we solve (54) subject to the boundary condition $w_0(0) = w_c$, obtaining

$$w_0(t) = w_c + (G + G_{\rm P})\left\{1 - \exp\left(-\frac{t}{2G_{\rm P}}\right)\right\}, \tag{55}$$

Then, setting $n = 1$ in (53), we find

$$w_1(t) = w_c + G - G_{\rm P} - e^{-\lambda}(G + G_{\rm P}) \exp\left(-\frac{t}{2G_{\rm P}}\right).$$

The second boundary condition $w_1(1/V) = w_c$ yields the desired approximation of the kinetic relation

$$G(V) = G_{\rm P} + \frac{(1 - e^{-\lambda})(G_{\rm S} - G_{\rm P})}{\exp(\frac{1}{2G_{\rm P}V}) - \exp(-\lambda)}. \tag{56}$$

Clearly, $G(V) \to G_{\rm P}$ as $V \to 0$ and $G(V)$ tends to the spinodal value $G_{\rm S} = 1/2$ as V goes to infinity, in agreement with (34). Note, however, that the

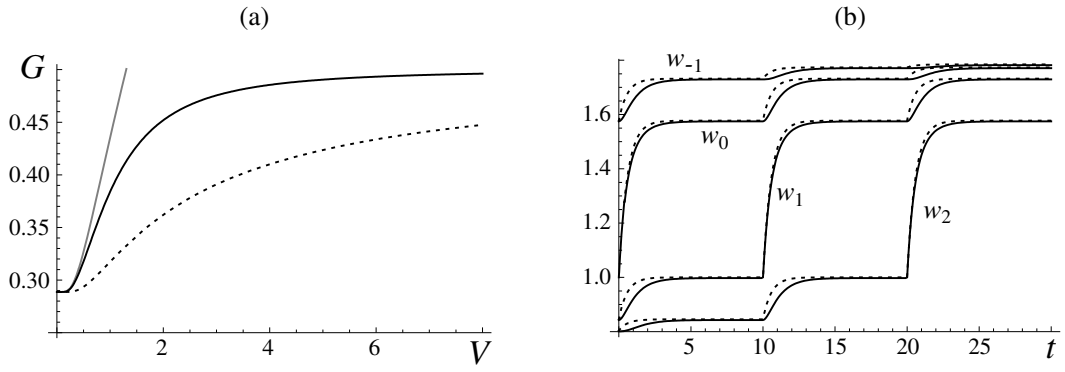

Fig. 5. (a) Kinetic relations $G(V)$: infinite-dimensional dynamics (solid curve), its small-velocity approximation (45) (grey curve) and $K = 1$ approximation (dotted curve). (b) Comparison of strain trajectories in the $K = 1$ reduced model (dotted curves) and in the original infinite-dimensional model (solid curves). Parameters: $V = 0.1$, $D = 0.5$, $w_c = 1$.

asymptotic behavior at small V, $G - G_{\rm P} \sim \exp(-\frac{1}{2G_{\rm P}V})$, differs from the asymptotics (45). This is not surprising since we have replaced the infinite-dimensional dynamical system by a single differential equation for $w_0(t)$.

The next step is to patch different segments of the dynamic trajectory into one by introducing a single order parameter. Recall that during each time period $k/V \le t \le (k+1)/V$ the active strain is $w_k(t)$, and the corresponding solution can be obtained by replacing n in the expressions above for $k = 0$ by $n - k$ and t by $t - k/V$. Introduce a new continuous monotonically increasing function

$$\begin{aligned}\nu(t) =& [Vt] + \frac{1 - \exp(-\frac{1}{2G_{\rm P}}(t - \frac{[Vt]}{V}))}{1 - \exp(-\frac{1}{2G_{\rm P}})} \\ =& [Vt] + \frac{G + G_{\rm P}}{(G_{\rm S} - G)(e^{\lambda} - 1)}\left\{1 - \exp\left(-\frac{1}{2G_{\rm P}}\left(t - \frac{[Vt]}{V}\right)\right)\right\},\end{aligned} \tag{57}$$

where $[\nu] = [Vt]$ and (56) was used to obtain the second equality. Note that $\nu(t)$ takes consecutive integer values at the beginning of each time period. It is exactly the dynamic extension of the parameter ν which we used to obtain the static PN landscape. In terms of this new "global" order parameter, we obtain the following expression for any active strain $w_{[\nu]}(t)$ (over the time period $[\nu]/V \le t \le ([\nu] + 1)/V$):

$$w_{[\nu]}(t) = w_c + (e^{\lambda} - 1)(G_{\rm S} - G)(\nu(t) - [\nu(t)]),$$

and hence time evolution of all strains can be written in terms of ν as

$$w_n(t) = w_c - 1/2 + G+$$
$$\begin{cases} 1 + \Big((e^\lambda - 1)(G_{\rm S} - G)(\nu(t) - [Vt]) - G - G_{\rm S}\Big)e^{\lambda(n-[Vt])}, & n \le [Vt] \\ \Big((e^\lambda - 1)(G_{\rm S} - G)(\nu(t) - [Vt]) - G + G_{\rm S}\Big)e^{-\lambda(n-[Vt])} & n \ge [Vt] + 1. \end{cases} \tag{58}$$

Note that although $\nu(t)$ is by construction a continuous function of time, the strain variables have jump discontinuities at $t = n/V$, $n = 1, 2 \ldots$, due to the fact that our approximation treats non-active strains as if they are equilibrated and neglects the corresponding dynamics. As a result, at the end of each time period we switch to the new active strain, and the old one has to increase its value in order to be in equilibrium with the new active point; the associated jumps can be computed explicitly:

$$[\![w_n]\!]_{t=(n+1)/V} = [\![w_0]\!]_{t=1/V} = w_0(1/V + 0) - w_0(1/V - 0) = 2\sinh\lambda(G - G_{\rm P}).$$

Now we are in a position to construct the global DPN potential $\Phi(\nu; G)$ which serves as a landscape for the overdamped dynamics of $\nu(t)$:

$$\dot\nu = -\alpha\Phi'(\nu; G). \tag{59}$$

The potential must be clearly piecewise quadratic and we can select the coefficients to ensure that the function (57) is the solution of (59). If we choose the mobility as $\alpha = 1/(4G_P^2)$ the resulting potential

$$\Phi(\nu; G) = G_{\rm P}\left((\nu - [\nu])^2 - \frac{2(G + G_{\rm P})}{(e^\lambda - 1)(G_{\rm S} - G)}\nu + [\nu]\right). \tag{60}$$

coincides with the equilibrium PN landscape at $G = G_{\rm P}$ (see Figure 3).

The one-dimensional dynamics (59) is compared to the full infinite-dimensional dynamics in Figure 5b. As expected, the evolution of the active strain is captured quite well, but there is a visible deviation from the actual values for the strains whose adjustment was assumed to be instantaneous. The corresponding kinetic relations are juxtaposed in Figure 5a.

One can see that the approximate model provides a good quantitative approximation of the exact kinetic relation until $V = 0.2$. At higher velocities it deviates substantially from the exact relation, although both tend to the same spinodal limit $G_{\rm S}$ at infinite V.

To obtain a better approximation, we need to consider more active points in the core region of the defect. From Figure 5b one can see that in each period the natural choice for the expanded set of order parameters would be w_{-1}, w_0 and w_1.

By minimizing the energy with respect to all other strain variables, we obtain

$$w_n = \begin{cases} w_c + G + 1/2 + (w_{-1} - w_c - G - 1/2)e^{\lambda(n+1)}, & n \leq -1 \\ w_0, & n = 0 \\ w_c + G - 1/2 + (w_1 - w_c - G + 1/2)e^{\lambda(1-n)} & n \geq 1. \end{cases} \tag{61}$$

Observe that the dynamics of $w_{-1}(t)$, $w_0(t)$ and $w_1(t)$ is not independent. Indeed, the three active points satisfy the dynamic equations

$$\begin{aligned} \dot{w}_{-1} &= D(w_0 - 2w_{-1} + w_{-2}) - w_{-1} + w_c + G + 1/2 \\ \dot{w}_0 &= D(w_1 - 2w_0 + w_{-1}) - w_0 + w_c + G + 1/2 \\ \dot{w}_1 &= D(w_2 - 2w_1 + w_0) - w_1 + w_c + G - 1/2 \end{aligned} \tag{62}$$

Substituting the expressions for w_2 and w_{-2} from (61) in (62), we obtain

$$\begin{aligned} \dot{w}_{-1} &= (-2D - 1 + e^{-\lambda}D)w_{-1} + Dw_0 + (w_c + G + 1/2)(1 + D(1 - e^{-\lambda})) \\ \dot{w}_0 &= (-2D - 1)w_0 + Dw_1 + Dw_{-1} + w_c + G + 1/2 \\ \dot{w}_1 &= (-2D - 1 + e^{-\lambda}D)w_{-1} + Dw_0 + (w_c + G - 1/2)(1 + D(1 - e^{-\lambda})) \end{aligned} \tag{63}$$

If we now compare the equations governing the dynamics of $w_{-1}(t)$ and $w_1(t)$, we see that they differ only by a constant term in the right hand side. This allows us to reduce the number of variables further and express the functions $w_{-1}(t)$ and $w_1(t)$ in terms of a single new variable $x(t)$. We write

$$w_{\mp 1}(t) = x(t) \pm \frac{1 + D(1 - e^{-\lambda})}{2(1 + D(2 - e^{-\lambda}))} = x(t) \pm \frac{1 - e^{-\lambda}}{2}, \tag{64}$$

where we have used (36) to obtain the second equality. We now have two variables: $w_0(t)$, describing the dynamics of the "center of mass" of the phase boundary, and $x(t)$, which describes the configuration of the core region. They must solve the following system of equations

$$\dot{w}_0 = (-2D - 1)w_0 + 2Dx + w_c + G + 1/2 \tag{65}$$

$$\dot{x} = (-2D - 1 + e^{-\lambda}D)x + Dw_0 + (w_c + G)(1 + D(1 - e^{-\lambda})). \tag{66}$$

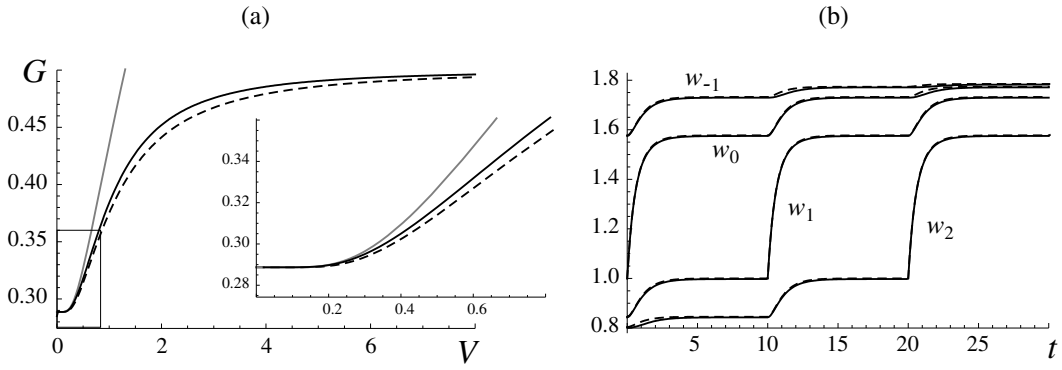

Fig. 6. (a) Kinetic relations $G(V)$: infinite-dimensional system (solid curve), its small-velocity approximation (45) (grey curve) and the $K = 2$ reduced system (dashed curve); (b) Comparison of the strain trajectories in the $K = 2$ model (dashed curves) and in the infinite-dimensional system model (solid curves). Parameters: $V = 0.1$, $D = 0.5$, $w_c = 1$.

This system constitutes our kinetic equation approximating the dynamics of the full infinite-dimensional system.

To reproduce traveling wave solutions of the original system the reduced system (65), (66), must be subjected to the following boundary conditions. First, we must require that

$$w_0(0) = w_c, \tag{67}$$

a condition that ensures that the 0th NN spring has just transformed to the new phase at $t = 0$. Second, we require that

$$w_1(1/V) = w_c,$$

or

$$x(1/V) = w_c + \frac{1 - e^{-\lambda}}{2}, \tag{68}$$

so that at $t = 1/V$ the first NN spring reaches the critical strain, marking the end of the period. Finally, periodicity requires that

$$w_1(0) = w_2(1/V).$$

We can now construct approximate kinetic relation generated by the $K = 2$ model. Using (61) at $n = 2$ together with (68), we can see that this boundary condition reduces to

$$w_1(0) = w_c - (G_{\rm S} - G)(1 - e^{-\lambda}),$$

or

$$x(0) = w_c - (G_{\rm S} - G)(1 - e^{-\lambda}) + \frac{1 - e^{-\lambda}}{2}. \tag{69}$$

Next, by solving the system (65), (66) subject to the initial conditions (67) and (69), we obtain

$$x(t) = w_c + G + e^{-\lambda}G_{\rm P} + \frac{e^{-\lambda}}{4}(c_1(1+\sqrt{1+8e^{2\lambda}})e^{r_1 t} + c_2(1-\sqrt{1+8e^{2\lambda}})e^{r_2 t})$$
$$w_0(t) = w_c + G + G_{\rm P} + c_1 e^{-r_1 t} + c_2 e^{-r_2 t}, \tag{70}$$

where

$$r_{1,2} = -\frac{e^{\lambda}}{4\sinh^2(\lambda/2)}\left(1 + \frac{1}{2}e^{-2\lambda}(1 \mp \sqrt{1+8e^{2\lambda}})\right) \tag{71}$$

(note that $r_2 < r_1 < 0$) and

$$c_1 = -\frac{(3+\sqrt{1+8e^{2\lambda}})(2G-1+e^{\lambda}(1+2G))}{4(1+e^{\lambda})\sqrt{1+8e^{2\lambda}}}$$
$$c_2 = -\frac{(\sqrt{1+8e^{2\lambda}}-3)(2G-1+e^{\lambda}(1+2G))}{4(1+e^{\lambda})\sqrt{1+8e^{2\lambda}}}.$$

The boundary condition (68) now yields the desired kinetic relation:

$$G(V) = \frac{G_{\rm P} + \frac{1-e^{-\lambda}}{4(1+e^{\lambda})\sqrt{1+8e^{2\lambda}}}\left((1+2e^{2\lambda}+\sqrt{1+8e^{2\lambda}})e^{r_1/V} + (\sqrt{1+8e^{2\lambda}}-2e^{2\lambda}-1)e^{r_2/V}\right)}{1 - \frac{e^{-\lambda}}{2\sqrt{1+8e^{2\lambda}}}\left((1+2e^{2\lambda}+\sqrt{1+8e^{2\lambda}})e^{r_1/V} + (\sqrt{1+8e^{2\lambda}}-2e^{2\lambda}-1)e^{r_2/V}\right)}. \tag{72}$$

First we notice that the approximate kinetic relation (72) satisfies the constraint $G(0) = G_{\rm P}$. Then, as V tends to infinity, $G(V) \to G_{\rm S} = 1/2$ with the asymptotics $G - G_{\rm s} \sim \exp(-|r_1|/V)$. The comparison of the approximate and exact kinetic relations is presented in Figure 6. One can see that in view of how few degrees of freedom are involved in the approximation, the agreement is remarkable, at least for small to moderate values of D (see Figure 7). At larger D (strong coupling limit) more active points need to be included, or rather the structure of the approximation must be changed due to close to continuum character of the model in this limit.

Our next goal is to introduce the global order parameter and to reformulate the dynamics in the form of a gradient flow on a two-dimensional DPN landscape. First recall that expressions (70), (64) and (61) define the strain trajectories $w_n(t)$ only over the time period $0 \le t \le 1/V$. The extension of this solution for $k/V \le t \le (k+1)/V$ is obtained by replacing n in the above formulas by $n-k$ and t by $t - k/V$. To patch together different periods we need to introduce a set of two order parameters that change continuously and monotonically with t. We denote these variables as $\tilde{\nu}_1(t)$ and $\tilde{\nu}_2(t)$ and define them by the conditions $[\tilde{\nu}_1(t)] = [\tilde{\nu}_2(t)] = [Vt]$, $w_{[Vt]}(t) = w_c + (\tilde{\nu}_1(t) - [Vt])(w_0(1/V) - w_c)$

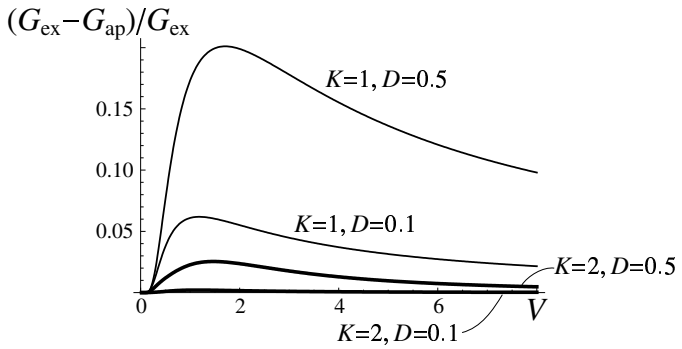

Fig. 7. The error in the approximation of the the exact kinetic relation $G_{\rm ex}(V)$ by the reduced models with $K = 1$ and $K = 2$ generating approximate kinetic relation $G_{\rm ap}(V)$.

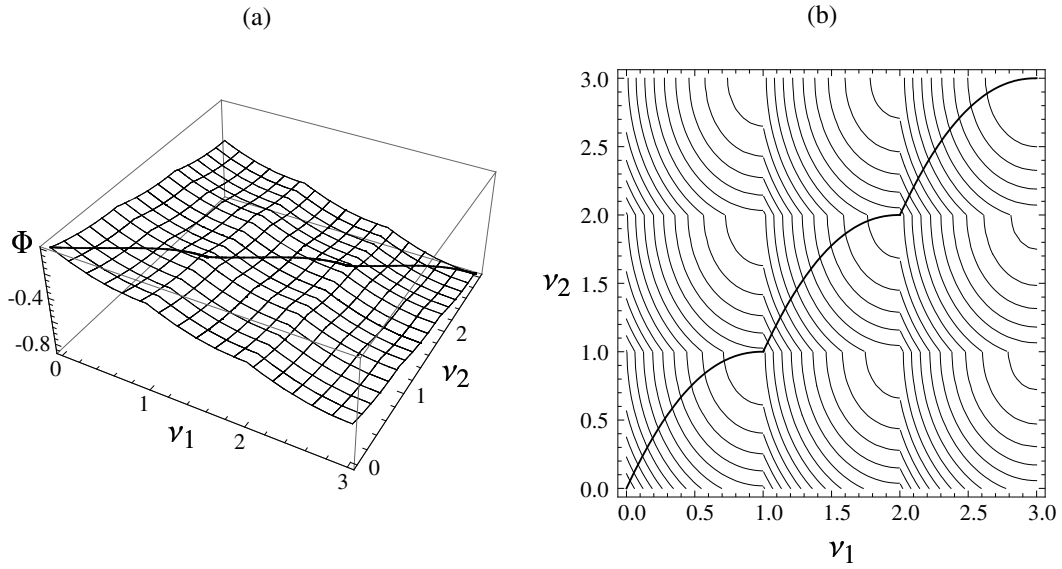

Fig. 8. (a) Two-dimensional energy landscape $\Phi(\nu_1, \nu_2)$. (b) Level sets of the energy along with the path of the effective particle $\boldsymbol{\nu}(t)$. Parameters: $V = 0.1$, $D = 0.5$, $w_c = 1$.

and $\tilde{x}(t) = x(0) + (\tilde{\nu}_2(t) - [Vt])(x(1/V) - x(0))$, where $\tilde{x}(t)$ is viewed as an extension of $x(t)$ to all $t \geq 0$. Under the assumption that $V = V(G)$ the dynamics of the vector field $\tilde{\nu}(t) = (\tilde{\nu}_1(t), \tilde{\nu}_2(t))$ can be represented as a gradient flow

$$\dot{\boldsymbol{\nu}} = -\tilde{\boldsymbol{\alpha}} \nabla \tilde{\Phi}(\tilde{\boldsymbol{\nu}}, \boldsymbol{G}) \tag{73}$$

where we introduced a mobility matrix $\tilde{\boldsymbol{\alpha}}$ and a two-dimensional effective DPN potential $\tilde{\Phi}(\tilde{\boldsymbol{\nu}}, G)$.

We can further simplify our *kinetic equation* (73) by diagonalizing the mobility matrix $\tilde{\boldsymbol{\alpha}}$. Observe that in (71) we have $|r_2| > |r_1| > 0$, so that the eigenvector $(\frac{e^{-\lambda}}{4}(\sqrt{1+8e^{2\lambda}}+1), 1)$ corresponding the eigenvalue r_2 is the slow direction, while the eigenvector $(\frac{e^{-\lambda}}{4}(1-\sqrt{1+8e^{2\lambda}}), 1)$ that corresponds to r_1 is the fast

direction. Thus we can introduce the *slow* variable

$$\nu_1(t) = [Vt] + \frac{1 - \exp(r_1(t - [Vt]/V))}{1 - \exp(r_1/V)} \tag{74}$$

and the *fast* variable

$$\nu_2(t) = [Vt] + \frac{1 - \exp(r_2(t - [Vt]/V))}{1 - \exp(r_2/V)}. \tag{75}$$

In terms of the new variables, the time evolution of all strains is given by

$$w_n(t) = \begin{cases} w_c + G + 1/2 + \{G_{\rm P} - 1/2 + \frac{1}{4}c_1(1 + \sqrt{1+8e^{2\lambda}})(1 - (1 - e^{-r_1/V})(\nu_1(t) - [Vt])) \\ \quad + c_2(1 - \sqrt{1+8e^{2\lambda}})(1 - (1 - e^{-r_2/V})(\nu_2(t) - [Vt]))\}e^{\lambda(n-[Vt])}, \quad n \le [Vt] - 1 \\ w_c + G + G_{\rm P} + c_1(1 - (1 - e^{-r_1/V})(\nu_1(t) - [Vt])) \\ \quad + c_2(1 - (1 - e^{-r_2/V})(\nu_2(t) - [Vt]))\}, \quad n = [Vt] \\ w_c + G - 1/2 + \{G_{\rm P} + 1/2 + \frac{1}{4}c_1(1 + \sqrt{1+8e^{2\lambda}})(1 - (1 - e^{-r_1/V})(\nu_1(t) - [Vt])) \\ \quad + c_2(1 - \sqrt{1+8e^{2\lambda}})(1 - (1 - e^{-r_2/V})(\nu_2(t) - [Vt]))\}e^{-\lambda(n-[Vt])}, \quad n \le [Vt] - 1. \end{cases} \tag{76}$$

The vector field $\boldsymbol{\nu}(t) = (\nu_1(t), \nu_2(t))$ satisfies

$$\dot{\boldsymbol{\nu}} = -\boldsymbol{\alpha}\nabla\Phi(\boldsymbol{\nu}, G), \tag{77}$$

where the mobility matrix $\boldsymbol{\alpha} = \mathrm{diag}(\alpha_1, \alpha_2)$ is now diagonal (here $\alpha_1 > 0$ and $\alpha_2 > 0$ are constants). The potential $\Phi(\nu_1, \nu_2; G)$ is piecewise quadratic; it depends on V and hence, through the kinetic relation $V = V(G)$ which can be obtained by inverting (72), on the driving force G. Using (74) and (75), we obtain

$$\begin{aligned} \Phi(\nu_1, \nu_2; G) = &-\frac{r_1}{2\alpha_1}\left\{(\nu_1 - [\nu_1])^2 - \frac{2}{1 - \exp(r_1/V(G))}\nu_1 + [\nu_1]\right\} \\ &-\frac{r_2}{2\alpha_2}\left\{(\nu_2 - [\nu_2])^2 - \frac{2}{1 - \exp(r_2/V(G))}\nu_2 + [\nu_2]\right\}. \end{aligned}$$

To determine the effective viscosities α_1 and α_2, we require that at $G_{\rm P}$ the DPN potential equals the relative Gibbs free energy of the system:

$$\Phi(\boldsymbol{\nu}; G_{\rm P}) = \mathcal{W}(\boldsymbol{\nu}; G_{\rm P}) - \mathcal{W}(\mathbf{0}; G_{\rm P}).$$

This yields

$$\alpha_1 = -\frac{r_1\sqrt{1+8e^{2\lambda}}}{(\sqrt{1+8e^{2\lambda}} + 3)G_{\rm P}}, \quad \alpha_2 = -\frac{r_1\sqrt{1+8e^{2\lambda}}}{(\sqrt{1+8e^{2\lambda}} - 3)G_{\rm P}} \tag{78}$$

and, finally,

$$\Phi(\nu_1,\nu_2;G) = \frac{(\sqrt{1+8e^{2\lambda}}+3)G_{\rm P}}{2\sqrt{1+8e^{2\lambda}}}\left\{(\nu_1-[\nu_1])^2 - \frac{2}{1-\exp(r_1/V(G))}\nu_1 + [\nu_1]\right\} + \frac{(\sqrt{1+8e^{2\lambda}}-3)G_{\rm P}}{2\sqrt{1+8e^{2\lambda}}}\left\{(\nu_2-[\nu_2])^2 - \frac{2}{1-\exp(r_2/V(G))}\nu_2 + [\nu_2]\right\}. \tag{79}$$

The DPN landscape $\Phi(\nu_1,\nu_2;G)$, along with the path of the effective particle, is shown in Figure 8. The comparison of strain trajectories in the two-dimensional reduced theory with the exact result shows the considerable improvement over the one-dimensional approximation. For instance, Figure 6b juxtaposes the evolution of strains near the phase boundary over the first three time periods at $V = 0.1$. One can see that as in the case $K = 1$ the evolution of the transforming element is followed closely over each time period; however, in the $K = 2$ case the dynamics of other, nontransforming elements is also captured extremely well.

Acknowledgements. This work was supported by the National Science Foundation grant DMS-0443928 (A.V.) and by the EU contract MRTN-CT-2004-505226 (L.T.).

References

Abeyaratne, R., Knowles, J., 1991. Kinetic relations and the propagation of phase boundaries in solids. Arch. Rat. Mech. Anal. 114, 119–154.

Arndt, M., Luskin, M., 2008. Error estimation and atomistic-continuum adaptivity for the quasicontinuum approximation of Frenkel-Kontorova model. Multiscale Modeling and Simulation 7, 147–170.

Braun, O. M., Kivshar, Y. S., 2004. The Frenkel-Kontorova model: concepts, methods and applications. Texts and monographs in physics. Springer-Verlag, Berlin Heidelberg.

Braun, O. M., Kivshar, Y. S., Zelenskaya, I. I., 1990. Kinks in the Frenkel-Kontorova model with long-range interparticle interactions. Physical Review B 41, 7118–7138.

Carpio, A., Bonilla, L. L., 2003. Depinning transitions in discrete reaction-diffusion equations. SIAM Journal of Applied Mathematics 63 (3), 1056–1082.

Celli, V., Flytzanis, N., 1970. Motion of a screw dislocation in a crystal. Journal of Applied Physics 41 (11), 4443–4447.

Fáth, G., 1998. Propagation failure of traveling waves in discrete bistable medium. Physica D 116, 176–190.

Flach, S., Kladko, K., 1996. Perturbation analysis of weakly discrete kinks. Phys. Rev. E 54, 2912–2916.

Furuya, K., de Almeida, A. M. O., 1987. Soliton energies in the standard map beyond the chaotic threshold. J. Phys. A 20, 6211–6221.

Gruner, G., Zawadowski, A., Chaikin, P. M., 1981. Nonlinear conductivity and noise due to charge-density-wave depinning in NbSe3. Phys. Rev. Lett 46, 511–515.

Gurtin, M. E., 1999. Configurational forces as basic concepts of continuum physics. Vol. 137 of Applied Mathematical Sciences. Springer-Verlag, New York.

Hobart, R., 1965. Peierls stress dependence on dislocation width. J. Appl. Phys. 36, 1944–1948.

Hobart, R., 1966. Peierls barrier analysis. J. Appl. Phys. 37, 3573–3576.

Ishibashi, Y., Suzuki, I., 1984. On the evaluation of the pinning (Peierls) energy of kinks due to discreteness of substrate lattices. J. Phys. Soc. Jpn. 53, 4250–4256.

Ishimori, Y., Munakata, T., 1982. Kink dynamics in the discrete Sine-Gordon system: a perturbational approach. J. Phys. Soc. Jpn. 51, 3367–3374.

Joos, B., 1982. Properties of solitons in the Frenkel-Kontorova model. Solid State Commun. 42, 709–713.

Kardar, M., 1998. Nonequilibrium dynamics of interfaces and lines. Phys. Rep. 301, 85–112.

Keener, J. P., 1987. Propagation and its failure in coupled systems of discrete excitable cells. SIAM Journal of Applied Mathematics 47 (3), 556–572.

Kladko, K., Mitkov, I., Bishop, A. R., 2000. Universal scaling of wave propagation failure in arrays of coupled nonlinear cells. Phys. Rev. Letters 84 (19), 4505–4508.

Kresse, O., Truskinovsky, L., 2003. Mobility of lattice defects: discrete and continuum approaches. Journal of the Mechanics and Physics of Solids 51, 1305–1332.

Kresse, O., Truskinovsky, L., 2007. Prototypical lattice model of a moving defect: the role of environmental viscosity. Izvestiya, Physics of the Solid Earth 43, 63–66.

Lazutkin, V. F., Schachmannski, I. G., Tabanov, M. B., 1989. Splitting of separatrices for standard and semistandard mappings. Physica D 40, 235–348.

Li, X., E, W., 2005. Multiscale modeling of the dynamics of solids and finite temperature. J. Mech. Phys. Solids 53, 1650–1685.

Maugin, G. A., 1993. Material Inhomogeneities in Elasticity. Vol. 3 of Applied Mathematics and Mathematical Computation. Chapman and Hall.

Pokrovsky, V. L., 1981. Splitting of commensurate-incommensurate phase transition. J. Phys. (Paris) 42 (6), 761–766.

Rice, J. R., Ruina, A. L., 1983. Stability of steady frictional slipping. Journal of Applied Mechanics 50, 343–349.

Ruina, A. L., 1985. Constitutive relations for frictional slip. In: Mechanics of

geomaterials. Numerical methods in Engineering. John Willey & Sons, New York, pp. 169–187.

Slemrod, M., 1983. Admissibility criteria for propagating phase boundaries in a van der Waals fluid. Archive for Rational Mechanics and Analysis 81, 301–315.

Slepyan, L. I., 1982. The relation between the solutions of mixed dynamical problems for a continuous elastic medium and a lattice. Soviet Physics Doklady 27 (9), 771–772.

Tadmor, E. B., Ortiz, M., Phillips, R., 1996. Quasicontinuum analysis of defects in solids. Phil. Mag. A 73, 1529–1563.

Truskinovsky, L., 1982. Equilibrium interphase boundaries. Soviet Physics Doklady 27, 306–331.

Truskinovsky, L., 1987. Dynamics of nonequilibrium phase boundaries in a heat conducting elastic medium. J. Appl. Math. Mech. 51, 777–784.

Truskinovsky, L., Vainchtein, A., 2003. Peierls-Nabarro landscape for martensitic phase transitions. Physical Review B 67, 172103.

Truskinovsky, L., Vainchtein, A., 2004. The origin of nucleation peak in transformational plasticity. Journal of the Mechanics and Physics of Solids 52, 1421–1446.

Truskinovsky, L., Vainchtein, A., 2005. Kinetics of martensitic phase transitions: Lattice model. SIAM Journal on Applied Mathematics 66, 533–553.

Truskinovsky, L., Vainchtein, A., 2008. Dynamics of martensitic phase boundaries: discreteness, dissipation and inertia. Continuum Mechanics and Thermodynamics 20 (2), 97–122.

Willis, C. R., El-Batanouny, M., Stancioff, P., 1986. Sine-Gordon kinks on a discrete lattice. I. Hamiltonian formalism. Phys. Rev. B 33, 1904–1911.